

# Photoelectron and photoion spectroscopy on atomic Lu in the region of the 5p excitation

 Ch. Gerth<sup>1</sup>, B. Kanngießner<sup>1</sup>, M. Martins<sup>2</sup>, P. Sladeczek<sup>1</sup>, K. Tiedtke<sup>1</sup>, and P. Zimmermann<sup>1,a</sup>
<sup>1</sup> Institut für Atomare und Analytische Physik, Technische Universität Berlin, Hardenbergstr. 36, 10623 Berlin, Germany

<sup>2</sup> Institut für Experimentalphysik, Freie Universität Berlin, Arnimallee 14, 14195 Berlin, Germany

Received: 2 September 1998 / Accepted: 17 September 1998

**Abstract.** The  $5p \rightarrow nd$  resonances of atomic Lu have been investigated by photoelectron and photoion spectroscopy using monochromatized synchrotron radiation in the vacuum ultraviolet energy region. The total photoion yield has been compared to calculations in which the extended Fano theory (Mies formalism) and the Hartree-Fock method were applied. The resonance structure is dominated by the spin-orbit splitting of the  $5p$  core hole. In the photoion yield spectra of singly and doubly charged ions a high fraction of  $\text{Lu}^{2+}$  ions has been found in the region of the  $5p^{-1}(^2P_{1/2})nd$  resonances. Photoelectron spectra, recorded in this resonance region, have been investigated with respect to deexcitation channels connected with  $\text{Lu}^{2+}$  ions. The  $5p^{-1}(^2P_{1/2})nd$  resonances predominantly autoionize by spin-flip into  $5p^{-1}(^2P_{3/2})\epsilon\ell$  states, which decay in the second step into  $\text{Lu}^{2+}$  final ionic states.

**PACS.** 32.80.Fb Photoionization of atoms and ions – 32.80.Hd Auger effects and innershell excitation or ionization

## 1 Introduction

Photoionization investigations with monochromatized synchrotron radiation in the energy range of the vacuum ultraviolet (VUV) provide information about the atomic structure and the dynamics of innershell photoprocesses ([1,2] and references therein). Photoabsorption, photoion and photoelectron spectroscopy have been established as versatile tools for the investigation of excitation and de-excitation processes.

The interest of photoionization investigations in the VUV region is concentrated on core resonances. As an example, prominent  $3p \rightarrow 3d$  resonances were found in the photoabsorption spectra of iron group ( $3d$ ) elements [2], which are caused by discrete transitions of the  $3p$  core-hole electron into the unfilled  $3d$  valence shell. These strong discrete transitions directly reveal the large radial overlap of the core hole and valence shell wavefunctions. Similar to the case of the  $3p \rightarrow 3d$  resonances, pronounced  $5p \rightarrow 5d$  resonances were observed in the photoabsorption spectra of lanthanides [3,4] and the photoion spectra of platinum group ( $5d$ ) elements [5]. Lutetium ( $Z = 71$ ) with the ground state configuration  $[\text{Xe}] 4f^{14}5d6s^2$  is assigned to the lanthanides as the last member. With respect to the one bound  $5d$  electron, Lu can also be related to the  $5d$  elements of the platinum group ( $Z = 72-78$ ), in which the successive filling of the  $5d$  subshell takes place.

The photoabsorption spectra of the  $3p \rightarrow 3d$  resonances of the  $3d$  elements change dramatically with increasing atomic number  $Z$ . Here, the coupling of the open  $3d$  subshell with the  $3p$  core hole gives rise to the complex resonance structure. On the other hand, in view of the  $5p \rightarrow 5d$  excitations of the heavy lanthanides Ho, Er, Tm, and Yb ( $Z = 67-70$ ), the photoabsorption [3,4] and photoion spectra [6,7] comprise two groups of resonances, which can be related to transitions from the  $5p_{3/2}^{-1}$  and  $5p_{1/2}^{-1}$  core-hole states. Therefore, the resonance structure is governed by the spin-orbit splitting of the  $5p$  core hole. For Lu with the bound  $5d$  electron in the ground state the question arises as to whether the  $5p \rightarrow nd$  resonance structure is dominated by the  $5p$  spin-orbit splitting or the coupling of the  $5p$  core hole with the open  $5d$  subshell.

In this paper, we report on photoion yield and photoelectron spectra of free Lu atoms in the energy region of the  $5p$  excitation and ionization. The structure of the  $5p$  excitations and the final ionic states after the decay process are analyzed by photoion spectroscopy. In order to demonstrate the most important excitation and decay channels, valence shell photoelectron spectra are taken in the resonance region. For the interpretation of the resonance structure, the total photoion yield is compared to calculations of the photoionization cross section where the extended Fano theory (Mies formalism) of autoionizing resonances was applied using atomic wavefunctions calculated with the Hartree-Fock (HF) method.

---

<sup>a</sup> e-mail: :pz@atom.physik.tu-berlin.de

## 2 Experiment

The measurements were performed with synchrotron radiation from the electron storage ring BESSY I in Berlin (Germany). The synchrotron radiation was dispersed by a toroidal grating monochromator (TGM) and focused on the atomic beam, which was produced in an effusion oven heated by electron impact [8]. The Lu metal was contained in a molybdenum crucible. For the thermal evaporation of Lu with a sufficient particle density in the interaction region ( $\approx 10^{11} \text{ cm}^{-3}$ ), a temperature of about 2000 K is necessary. At this temperature, the thermal population of the metastable state  $5d6s^2 \ ^2D_{5/2}$ , which lies 0.25 eV above the ground state  $5d6s^2 \ ^2D_{3/2}$ , has to be considered. 75% of the Lu atoms are in the  $^2D_{3/2}$  ground state and 25% are in the  $^2D_{5/2}$  state.

The photoion spectra were recorded at the beamline TGM 4 with a resolving power of  $E/\Delta E \approx 200$ . The photoions were extracted from the interaction region by short electric pulses, which also were used as start pulses in a standard time-of-flight measurement with a Wiley-McLaren type spectrometer [9]. By setting appropriate time windows for the stop pulses from the ion detector, the photoion yield spectra of singly and doubly charged ions were measured simultaneously as a function of the photon energy.

The photoelectron spectra were recorded with the use of a cylindrical mirror analyzer (CMA) at the undulator beamline TGM 5. The resolving power achieved with the TGM 5 was  $E/\Delta E \approx 500$ , whereas the energy resolution of the CMA was 1.0% of the pass energy of the analyzed electrons. The CMA only accepted electrons with an angle of emission close to the magic angle of  $54.7^\circ$  relative to the polarization axis of the synchrotron radiation. The photoelectron spectra were recorded at fixed photon energies  $h\nu$  while scanning the pass energy of the CMA. All spectra were corrected for the analyzer transmission. For the calibration of the binding energy scale, we used the Lu II  $6s^2 \ ^1S_0$  photoline [10]. The accuracy for the binding energy scale amounts to  $\pm 0.1$  eV.

## 3 Results and discussion

Figure 1a shows the photoion yield spectra of  $\text{Lu}^+$ ,  $\text{Lu}^{2+}$ , and the sum  $\text{Lu}^+ + \text{Lu}^{2+}$  in the photon energy range between 25 eV and 45 eV. The conspicuous feature of the total photoion yield ( $\text{Lu}^+ + \text{Lu}^{2+}$ ) is the distinct division into two different groups of resonances: one group of sharp resonances between 29 eV and 33 eV and another group of broader and asymmetric resonances between 35 eV and 40 eV. This resonance structure bears a strong resemblance to the corresponding structures of Ho, Er, Tm, and Yb [3]. In view of the separated contributions of singly and doubly charged photoions, it is obvious that the group of the broader resonances between 35 eV and 40 eV decays predominantly into  $\text{Lu}^{2+}$  final states. In order to illustrate the relative proportion of  $\text{Lu}^{2+}$  final states, the ratio  $\text{Lu}^{2+}/\text{Lu}^+$  is depicted in Figure 1b. The ratio starts with values of about 0.3 below

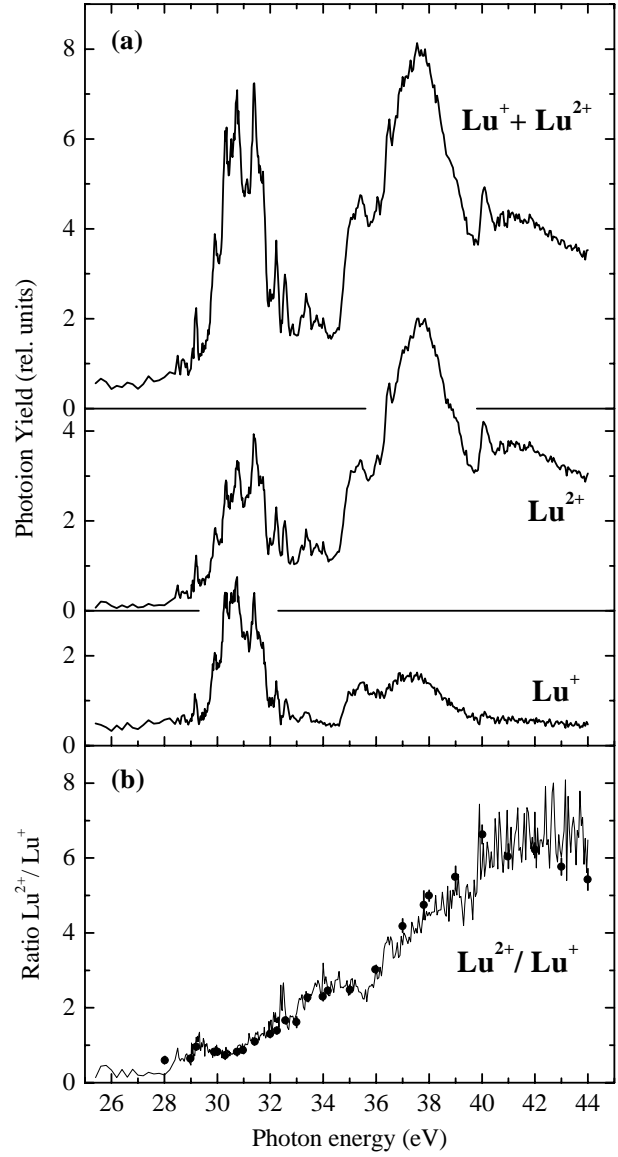


**Fig. 1.** (a) Photoion yield spectra of atomic Lu in the energy region of the  $5p$  excitation, showing the yields of  $\text{Lu}^+$  and  $\text{Lu}^{2+}$  and the total photoion yield ( $\text{Lu}^+ + \text{Lu}^{2+}$ ). (b) Ratio of singly and doubly charged ions.

28 eV, increases to a value of about 1 in the first group of resonances, and then rises nearly continuously to values of about 6 at 40 eV. The same pronounced increase in the ion ratio was found in the ion spectra [6, 7] of the lanthanides Ho, Er, Tm, and Yb.

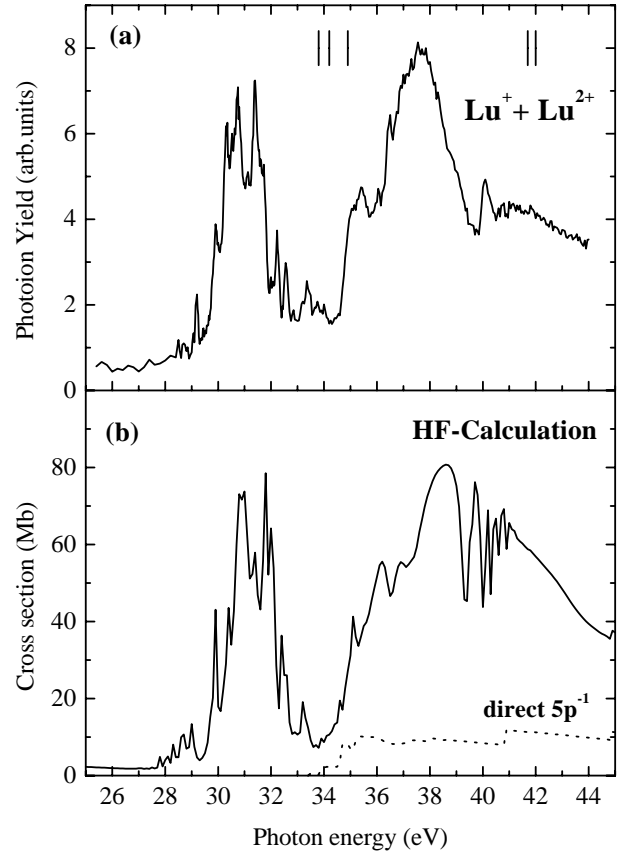
For a deeper understanding of the resonance structure in the photoion yield spectra, we performed calculations of the photoionization cross-section of Lu in this energy region. As initial states, both thermally populated fine-structure components  $^2D_{3/2}$  and  $^2D_{5/2}$  have to be considered (see Sect. 2). Due to the near degeneracy of the  $5d$  and  $6s$  orbitals, both initial states were calculated with the configurations  $5d6s^2$  and  $5d^26s$  to account for configuration interaction. For the excited discrete states,

**Table 1.** Initial and final state configurations included in the HF calculation of the photoionization cross-section.

Initial states	Final states	
	Discrete	Continuum
$5p^6 5d 6s^2$	$5p^5 5d^2 6s^2$	$5p^6 6s^2 \epsilon p, f$
$5p^6 5d^2 6s$	$5p^5 5d^3 6s$	$5p^6 5d 6s \epsilon p, f$
	$5p^5 5d 6s^2 6d$	$5p^6 5d^2 \epsilon p, f$
	$5p^5 5d 6s^2 7d$	$5p^6 6s 6d \epsilon p, f$
	$5p^5 5d 6s^2 8d$	$5p^6 6s 7d \epsilon p, f$
		$5p^6 6s 8d \epsilon p, f$
		$5p^6 5d 6d \epsilon p, f$
		$5p^6 5d 7d \epsilon p, f$
		$5p^6 5d 8d \epsilon p, f$
		$5p^5 5d 6s^2 \epsilon s, d$
		$5p^5 5d^2 6s \epsilon s, d$
		$5p^5 5d^3 \epsilon s, d$

the configuration  $5p^5 5d^2 6s^2$  for the transitions from  $5d 6s^2$ , and the configuration  $5p^5 5d^3 6s$  for the transitions from  $5d^2 6s$  were considered. In comparison to the  $5p \rightarrow 5d$  transitions, the  $5p \rightarrow 6s$  transitions are much weaker and were neglected in the calculations. The excited discrete states decay by the emission of a  $5d$  or  $6s$  electron into the continuum states  $5p^6 6s^2 \epsilon p, f$ ,  $5p^6 5d 6s \epsilon p, f$  or  $5p^6 5d^2 \epsilon p, f$ . The interference with the direct ionization of the  $5d$  or  $6s$  electrons into the same continuum states causes the asymmetrical Fano resonances [11]. Especially with respect to the production of doubly charged photoions  $\text{Lu}^{2+}$ , the ionization of the  $5p$  electrons has to be considered. Therefore, the continuum states  $5p^5 5d 6s^2 \epsilon s, d$ ,  $5p^5 5d^2 6s \epsilon s, d$ , and  $5p^5 5d^3 \epsilon s, d$  were also taken into account. The atomic wavefunctions were calculated with the Hartree-Fock method with relativistic corrections with the use of the Cowan code [12].

The resonances were calculated for both initial states  $^2D_{3/2}$  and  $^2D_{5/2}$  with all possible transitions  $J = 3/2 \rightarrow J' = 1/2, 3/2, 5/2$  and  $J = 5/2 \rightarrow J' = 3/2, 5/2, 7/2$ . Then, the resulting partial photoionization cross-sections were summed according to the thermal population of the initial states with a ratio of  $^2D_{3/2}:^2D_{5/2} = 3:1$  (see Sect. 2). The calculations were performed with various degrees of complexity. First, only the resonances due to the  $5p \rightarrow 5d$  transitions were considered and, secondly, transitions to higher Rydberg states  $5p \rightarrow nd$  with  $n = 6, 7, 8$  were included. The calculations showed that a proper description of the resonances requires the inclusion of transitions to higher Rydberg states. The different initial and final state configurations which were included in the calculation of the photoionization cross-section are summarized in Table 1. Parallel to the problem of higher Rydberg members one has to bear in mind that the resonances may overlap and cannot be regarded as independent Fano resonances but can interact with each other *via* the coupling of the corresponding continua. Therefore, we had

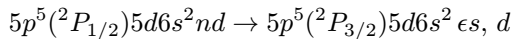
**Fig. 2.** (a) Total photoion yield spectrum ( $\text{Lu}^+ + \text{Lu}^{2+}$ ) of atomic Lu. The thresholds for the direct  $5p$  photoionization taken from reference [14] are included as vertical bars. (b) Theoretical photoionization cross-section of Lu calculated with the Mies formalism and the Hartree-Fock method. The configurations included in the calculation are summarized in Table 1.

to apply the extended Fano theory (Mies formalism) [13], where the interaction of many discrete with many continuum states is taken into consideration.

A comparison between experiment and theory is given in Figure 2. The measured total photoion yield is depicted in the upper part. The vertical bars mark the thresholds for the direct  $5p$  ionization, which were determined from a  $5p$  photoelectron spectrum of atomic Lu [14]. The calculated total photoionization cross-section is displayed in the lower part of Figure 2 together with the partial cross-section of the direct  $5p$  ionization. The overall agreement between experiment and theory is fairly good. Both spectra show the distinct characteristic of two groups of resonances and, furthermore, both spectra are strikingly similar to the corresponding spectra of Ho, Er, Tm, and Yb [3]. Strong transitions to Rydberg members of  $5p^5 6s^2 nd$  with  $n = 6-8$  have been identified in Yb [3,4]. However, the resonance structure of Lu is much more complex than that of the preceding element Yb, since the additional  $5d$  electron leads to a non-vanishing total orbital angular momentum  $^2D$  in the ground state and, thus, a larger number of resonance states can be excited. Owing to the

large number of overlapping resonances, a definite assignment for the resonances can not be given in the case of Lu. In contrast to Lu, the corresponding iron group element Sc ( $3d4s^2$ ), which is the first atom with a bound  $3d$  electron in the ground state, shows one broad  $3p \rightarrow 3d$  resonance, on which several smaller resonances are superimposed. The number and energy positions of these resonances reflect the multiplet splitting of the  $3p^5 3d^2 4s^2$  states, for which the LS coupling scheme was found to be appropriate to describe the splitting [2].

Due to the strong resemblance of the total photoion yield of Lu with the photoabsorption spectrum of Yb, the two groups of resonances can principally be ascribed to excitations from the  $5p^{-1}$  ( $^2P_{3/2}$ ) and  $5p^{-1}$  ( $^2P_{1/2}$ ) core hole states. Thus, the first group of resonances corresponds to excitations into  $5p^5(^2P_{3/2})5d6s^2nd$  ( $n \geq 5$ ) states, and the limits for the Rydberg transitions are given by the first  $5p$  ionization thresholds at about 34 eV. The resonances between 35 eV and the ionization thresholds at 41 eV mainly belong to excitations into  $5p^5(^2P_{1/2})5d6s^2nd$  ( $n \geq 5$ ) states. The stronger and more asymmetrical broadening of these resonances is well-reproduced by the calculations, where the interaction of many discrete with many continuum states is taken into account, as discussed above. This indicates prominent interaction of the Rydberg states with the continuum states  $5p^5(^2P_{3/2})5d6s^2$ . Since the Rydberg states lie entirely above the  $5p^5(^2P_{3/2})$  thresholds, autoionization by the spin-flip mechanism such as



becomes possible. The subsequent Auger decay of the Lu II  $5p^5(^2P_{3/2})5d6s^2$  states leads to Lu $^{2+}$  final ionic states. This decay mechanism has already been proposed by Tracy [3] as the dominant deexcitation process for the corresponding resonances of Yb.

To underpin this finding, a series of photoelectron spectra was recorded in the resonance region. The spectra are shown in Figure 3. Each spectrum is independently and arbitrarily normalized, so that comparisons of the relative intensities between different spectra are not meaningful. The correction for the transmission of the electron analyzer is only reliable for kinetic energies above 8 eV or binding energies below  $h\nu - 8$  eV, respectively. Energy positions indicated by vertical bars are taken from optical reference data [10]. The  $5d^{-1} \ ^1S$  and  $6s^{-1} \ ^1,^3D$  photoelectron lines are accompanied by satellite lines, which can be ascribed to Lu II  $5d^2$  states. In contrast to Sc, where the  $3d$  electron is more tightly bound than the  $4s$  electron, the  $5d^{-1}$  photoelectron line of Lu has a lower binding energy than the  $6s^{-1}$  photoline. The  $4f^{-1}$  photoelectron lines at binding energies between 15 eV and 18 eV are split by spin-orbit interaction into the two main components  $4f_{7/2}^{-1}$  and  $4f_{5/2}^{-1}$ . The  $4f^{-1}$  photoelectron lines might be superimposed by Lu II  $6snd$  and  $5dnd$  satellite lines with  $n \geq 6$ . The intensities of the photoelectron lines strongly vary with the photon energy, which is most obvious for the main  $5d$  and  $6s$  photoelectron lines. The  $5d^{-1}$ ,  $6s^{-1}$  and  $4f^{-1}$  photoelectron lines, lying below the lowest

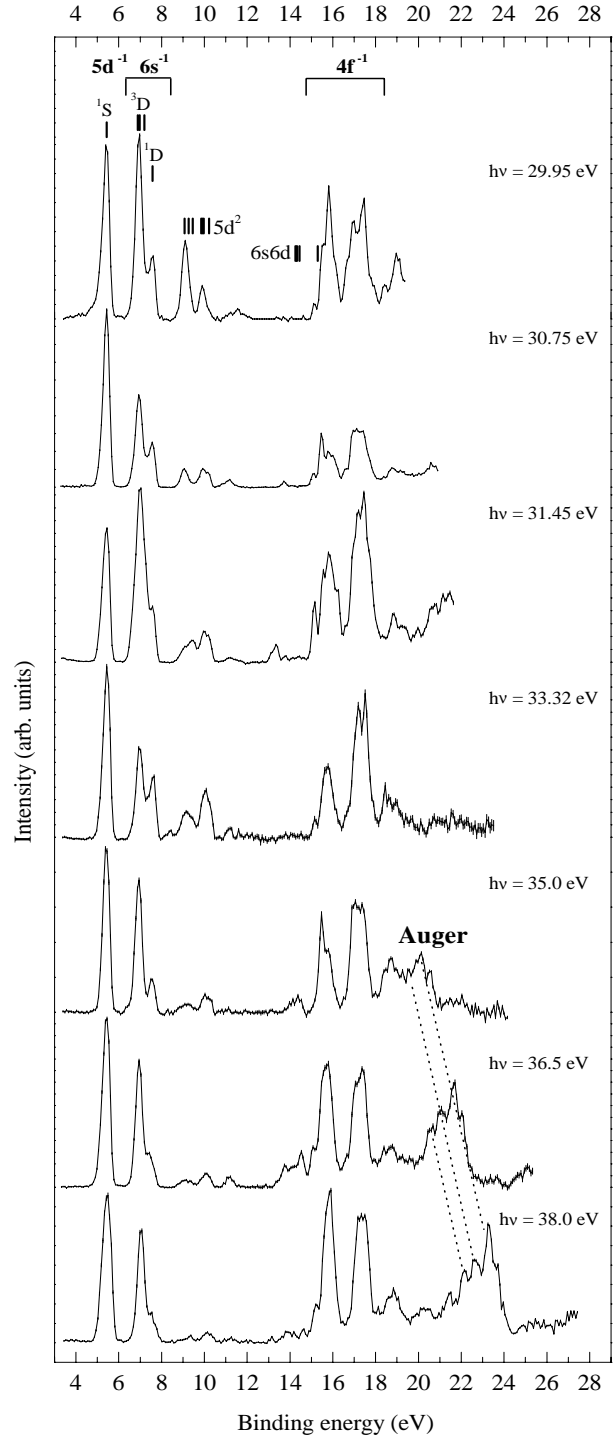


**Fig. 3.** Photoelectron spectra of atomic Lu recorded in the region of the  $5p \rightarrow nd$  resonances at photon energies between 29 eV and 38 eV. Energy levels of several Lu II states taken from optical data [10] are marked with vertical bars.

$2+$  threshold at  $19.31 \pm 0.37$  eV [10], are connected with Lu $^{+}$  final ionic states. At still higher binding energies a group of lines is clearly discernible for photon energies above 35 eV which shifts towards higher binding energies with increasing photon energy. By their energy shift these lines can be identified as Auger lines. The kinetic energies

**Table 2.** Experimentally observed Auger lines. The kinetic energies were determined from electron spectra recorded in the  $5p \rightarrow nd$  resonances between 36 eV and 40 eV. The uncertainty of the kinetic energies amounts to  $\pm 0.1$  eV.

Line No.	Kinetic energy (eV)	Final state Lu III
1	13.35	$5p^6 5d^2 D$
2	13.77	$5p^6 5d^2 D$
3	14.08	$5p^6 6s^2 S, 5p^6 5d^2 D$
4	14.47	$5p^6 6s^2 S, 5p^6 5d^2 D$
5	14.83	$5p^6 6s^2 S, 5p^6 5d^2 D$
6	15.44	$5p^6 6s^2 S, 5p^6 5d^2 D$
7	15.95	$5p^6 6s^2 S, 5p^6 5d^2 D$

of these Auger lines, determined from the photoelectron spectra, are given in Table 2. From their kinetic energies, these Auger lines can be related to decay processes  $5p^5(^2P_{3/2})5d6s^2 \rightarrow 5p^6 6s^2 S_{1/2} \epsilon \ell$  and  $5p^6 5d^2 D_{3/2,5/2} \epsilon \ell$ . Since the direct  $5p$  photoionization is one order of magnitude smaller than the resonant excitations (see Fig. 2b), the Auger lines can be attributed to the subsequent decay of resonantly excited  $5p^{-1} (^2P_{1/2})$  states, which are autoionizing by a spin flip to  $5p^{-1} (^2P_{3/2})$  states in the first step of the decay. Due to the quite similar energy spacing of the initial and final states, the Auger lines overlap considerably and a definite assignment cannot be made.

In conclusion, the  $5p \rightarrow nd$  resonances of atomic Lu are dominated by the spin-orbit splitting of the  $5p^{-1}$  core hole resulting in two completely separated groups of resonances, which correspond to excitations from the  $5p^{-1} (^2P_{3/2})$  and  $5p^{-1} (^2P_{1/2})$  core-hole states. Thus, Lu fits well in the trend of the heavy lanthanides Ho, Er, Tm, and Yb [3, 6, 7]. The influence of the bound  $5d$  electron in the ground state configuration of Lu is comparably small. This is in contrast to the  $3d$  elements, where the  $3p-3d$  electrostatic interaction governs the  $3p \rightarrow 3d$  resonances. The resonances which correspond to excitations into the states  $5p^{-1} (^2P_{1/2})nd$  lie entirely above the lowest Lu II  $5p^{-1} (^2P_{3/2})$  thresholds. Therefore, these resonantly excited Rydberg states are energetically allowed to

autoionize by a spin-flip into  $5p^{-1} (^2P_{3/2})\epsilon \ell$  states, where the spin of the core hole changes but the core hole itself remains unfilled. The subsequent Auger decay of the Lu II  $5p^{-1} (^2P_{3/2})$  states into  $\text{Lu}^{2+}$  final states results in a steep increase of the  $\text{Lu}^{2+}$  signal in the photoion yield spectra within the resonance region. The detection of resonantly enhanced Auger lines in the electron spectra corroborate the significant contribution of the two-step decay for the  $5p^{-1} (^2P_{1/2})nd$  resonances into  $\text{Lu}^{2+}$  final states.

The authors thank M. Groen and H. Heinrich for their help during the measurements and the staff at BESSY for their assistance. Many fruitful discussions with Dr. A. Verweyen of the II. Institut für Experimentalphysik, Universität Hamburg are acknowledged with pleasure. The authors are grateful to L. Bennett for comments and suggestions. Financial support was received from the Deutsche Forschungsgemeinschaft (Zi 183/13-2). This work was carried out with partial support of the European Union under the HCM programme.

## References

1. V. Schmidt, Rep. Prog. Phys. **55**, 1483 (1992).
2. B. Sonntag, P. Zimmermann, Rep. Prog. Phys. **55**, 911 (1992).
3. D.H. Tracy, Proc. R. Soc. Lond. A. **357**, 485 (1977).
4. M.W.D. Mansfield, M.A. Baig, J. Phys. B: At. Mol. Opt. Phys. **26**, 2273 (1993).
5. M. Martins, P. Sladeczek, K. Tiedtke, P. Zimmermann, Eur. Phys. J. D **1**, 47 (1998).
6. D.M.P. Holland, K. Codling, R.N. Chamberlain, J. Phys. B: At. Mol. Phys. **14**, 839 (1981).
7. Ch. Dzionk, W. Fiedler, M. van Lucke, P. Zimmermann, Phys. Rev. A **41**, 3572 (1990).
8. K.J. Ross, B. Sonntag, Rev. Sci. Instrum. **66**, 4409 (1995).
9. W. Wiley, I. McLaren, Rev. Sci. Instrum. **26**, 1150 (1955).
10. W.C. Martin, R. Zabulas, L. Hagen, *Atomic Energy Levels – The Rare Earth Elements* (U.S. Government Printing Office, Washington D.C., 1978).
11. U. Fano, Phys. Rev. **124**, 1866 (1961).
12. R.D. Cowan, *The Theory of Atomic Structure and Spectra* (Berkeley, CA: University of California Press, 1981).
13. F.H. Mies, Phys. Rev. **175**, 164 (1968).
14. Ch. Gerth, M. Martins, K. Godehusen, B. Kanngießner, P. Zimmermann, J. Phys. B (submitted).